Journal of Alloys and Compounds 509 (2011) 8283–8288

Contents lists available at ScienceDirect

Journal of Alloys and Compounds

journal homepage: www.elsevier.com/locate/jallcom

Study of non-magnetic iron mononitride thin films

Mukul Gupta[a,*], Akhil Tayal[a], Ajay Gupta[a], V.Raghavendra Reddy[a], M. Horisberger[b], J. Stahn[c]

[a] UGC-DAE Consortium for Scientific Research, University Campus, Khandwa Road, Indore 452 001, India
[b] Laboratory for Developments and Methods, Paul Scherrer Institut, CH-5232 Villigen PSI, Switzerland
[c] Laboratory for Neutron Scattering, Paul Scherrer Institut, CH-5232 Villigen PSI, Switzerland

ARTICLE INFO

Article history:
Received 18 April 2011
Received in revised form 27 April 2011
Accepted 28 April 2011
Available online 24 May 2011

Keywords:
Magnetic films and multilayers
Nitride materials
Vapor deposition
Microstructure
Mössbauer spectroscopy

ABSTRACT

Iron mononitride, FeN, is known to exist in different phases and there is a debate on the exact crystal type and the coexistence of these phases. We prepared single phase iron mononitride thin films by magnetron sputtering with various deposition rates (sputtering power) and investigated them with X-ray diffraction, neutron reflectometry and low temperature and high magnetic field Mössbauer spectroscopy. It was observed that with an increase in the sputtering power a more disordered structure is formed while the local chemical environment of iron remains unaffected. The low temperature and high magnetic field Mössbauer spectroscopy measurements confirmed that the FeN phase is paramagnetic at 5 K and an applied magnetic field of 5 T reflects magnetic splitting caused by the applied field. The obtained results are discussed in this study.

1. Introduction

Iron nitrides are interesting materials both from fundamental and application point of view. The magnetic iron nitrides (N at.% <25) are well-known due to their chemical inertness and mechanically hard surfaces [1]. This, together with their intrinsic magnetic properties, makes them a suitable material as an alternative to pure Fe in devices such as reading heads for magnetic storage devices [2]. The first phase diagram of iron nitrides was given by Jack [3,4] and has been reviewed consistently with the most recent appearing in 2011 [5]. After the discovery of a giant magnetic moment in α''-$Fe_{16}N_2$ (~11 at.% of nitrogen) by Kim and Takahashi [6], the interest in this compound grew immensely. The existence of the giant magnetic moment was confirmed later in 1990 [7]. Still, this compound remain controversial both from experimental and theoretical points of view (see e.g. [8] and references therein). With increasing the at.% N around to 20%, γ'-Fe_4N phase is formed which has a well-defined magnetic properties and crystal structure [9]. Very recently the γ'-Fe_4N phase has received a lot of interest due to its chemical inertness and mechanically hard surfaces making it a suitable alternative to pure Fe in magnetic devices [9–14]. Between 25 and 33 at.% N the iron nitride phases are known as ϵ-Fe_xN ($2 \leq x \leq 3$), as N at.% increases from 25% to 33% the phase changes from ferromagnetic Fe_3N to paramagnetic Fe_2N at room temperature. At about 33.3 at.% N the phase formed is ζ-Fe_2N [2,15].

On further increasing the nitrogen content to about 50%, iron mono-nitride (FeN) phase is formed. This is a non-magnetic compound and has been prepared in the form of thin films, only. FeN is known to exist mainly in the two phases with fcc structures: γ''-FeN with ZnS-type structure (lattice constant $a = 0.433$ nm) and γ'''-FeN with NaCl type structure (lattice constant $a = 0.450$ nm). A third phase called as γ_4 with lattice constant $a = 0.866$ nm was also observed [16]. Recently non-magnetic iron mononitrides have emerged as a promising material in spintronics applications [10–12]. A controlled annealing of FeN produces the γ'-Fe_4N phase and thus provides a source of spin injection for semiconductors or diluted magnetic semiconductors [17]. In addition the only N-rich compound, Fe_3N_4 having cubic spinel structure was theoretically predicted [18,19], though has not been evidenced experimentally so far.

Since the first preparation of γ'''-FeN by Oueldennaoua et al. [20] and γ''-FeN by Nakagawa et al. [21], several attempts were made to prepare and characterize thin films of γ''/γ'''-FeN [22–34]. Most of the studies concluded that both γ'' and γ''' phases of FeN coexist. However their coexistence remain controversial. The theoretical studies in iron mononitride predict that the lattice parameter of FeN in the NaCl structure should be between 0.39 and 0.42 nm, which is considerably lower than the experimentally obtained value of 0.45 nm [35,36]. In recent studies the existence of the γ'''-FeN phase in the NaCl-type structure was questioned [10,11,33], and concluded that the γ'''-FeN compound should have ZnS-type structure.

In the present work our aim is to study the structural and magnetic properties of iron mononitride thin films prepared using dc-magnetron sputtering. In the literature iron mononitride thin

* Corresponding author. Tel.: +91 731 246 3913; fax: +91 731 246 5437.
E-mail addresses: mgupta@csr.res.in, dr.mukul.gupta@gmail.com (M. Gupta).

0925-8388/$ – see front matter © 2011 Elsevier B.V. All rights reserved.
doi:10.1016/j.jallcom.2011.04.139

films have been deposited mainly by using a gas mixture of Ar + N_2, whereas in the present work we used pure N_2 as sputtering gas. This ensures that iron atoms get sputtered by nitrogen atoms and therefore the reaction probability increases to maximum and chances that the unreacted iron atoms also present in the deposited film can be ruled out completely. Further we increased the deposition rates by increasing the sputtering power and studied the effect of sputtering power on the structural and magnetic properties of deposited iron mononitride thin films. It was found that by increasing the sputtering power the grain size decreases while the local chemical environment of Fe atoms remains unaffected even at 5 K. The obtained results are presented and discussed in the following sections.

2. Experimental

Iron nitride thin films were prepared at room temperature using a direct current (dc)-magnetron sputtering technique on Si substrates. The samples were deposited using pure nitrogen as sputtering gas at a flow rate of 10 standard cubic centimeter per minute (sccm). A base pressure of $\approx 1\times10^{-7}$ mbar was achieved prior to deposition. During the deposition the partial pressure in the chamber was $\approx 4\times10^{-3}$ mbar. Pure Fe targets of 75 mm diameter were sputtered using a power of 50, 100 and 200 W. Before deposition the vacuum chamber was repeatedly flushed with nitrogen gas so as to minimize the possible contamination of trapped gases in the vacuum chamber. The targets were pre-sputtered for about 5 min in order to remove possible surface contaminations.

During the sample preparation we kept the deposition time constant and varied sputtering power at 50, 100 and 200 W. The obtained deposition rates are: 6.9 nm/min at 50 W; 7.7 nm/min at 100 W and 9.5 nm/min at 200 W. This indicates that the deposition rates increase linearly with an increase in sputtering power. This dependence can be easily understood in terms of Langmuir–Child relationship. The ion (here nitrogen) flux (J_{ion}) and its average kinetic energy (KE_{av}) are related to a dc glow discharge [37]:

$$J_{ion} \propto V_{dc}^{3/2} \quad \text{and} \quad KE_{av} \propto V_{dc} \tag{1}$$

Therefore both ion flux and average kinetic energy of atoms results in an increased glow discharge which in turn results in an increased deposition rate.

The structural and magnetic characterizations of the samples were carried out with following methods: (i) X-ray diffraction (XRD) using a standard X-ray diffractometer equipped with Cu K-α X-rays. (ii) Atomic force microscopy (AFM) measurements were carried out in samples deposited at sputtering power of 100 W and 200 W. (iii) Neutron reflectivity (NR) measurements were performed at the Apparatus for Multi Optional Reflectometry (AMOR) at SINQ/PSI, Switzerland [38] in the time-of-flight mode. (iv) Conversion electron Mössbauer spectroscopy (CEMS) measurements were carried out at room temperature using a ^{57}Co source embedded in a rhodium matrix. The CEMS measurements were carried out in the as-deposited samples and after annealing them at temperatures of 423 K, 523 K and 623 K. (v) The Mössbauer spectroscopy (MS) measurements were also performed in transmission mode at 300 K, 40 K and 5 K at 0 T and at 5 K at 5 T. The external magnetic field applied parallel to the gamma rays (using JANIS SuperOptiMag) superconduction magnet. The CEMS and MS patterns were calibrated to the hyperfine field of ^{57}Fe at room temperature. The conversion electrons were detected by a proportional counter having continuous flow of a helium–methane (5% methane balance helium) gas mixture.

3. Results and discussion

3.1. X-ray diffraction and atomic force microscopy

Fig. 1 shows the XRD pattern of the samples deposited using sputtering power of 50, 100 and 200 W. The peaks can be indexed to a fcc structure with a lattice constant $a = 0.453$ nm for 50 W, 0.454 nm for 100 W for the (1 1 1) reflection. The lattice constant values for 50 and 100 W matches well with a value of $a = 0.455$ nm obtained by Jouanny et al. [33] for iron mononitride having the γ'''-FeN phase with ZnS-type structure. The pattern corresponding to the sample prepared at sputtering power of 50 W and 100 W are almost identical but that of 200 W has lesser relative intensity and larger line widths. Therefore it is not possible to determine the value of a precisely for the sample deposited using sputtering power of 200 W. However, the line width of the diffracted pattern can be used to calculate the grain size of the diffracting specimen in the direction perpendicular to the plane of the film, using the Scherrer formula, [39] $t = 0.9\lambda/b\cos\theta$, where t is the grain size,

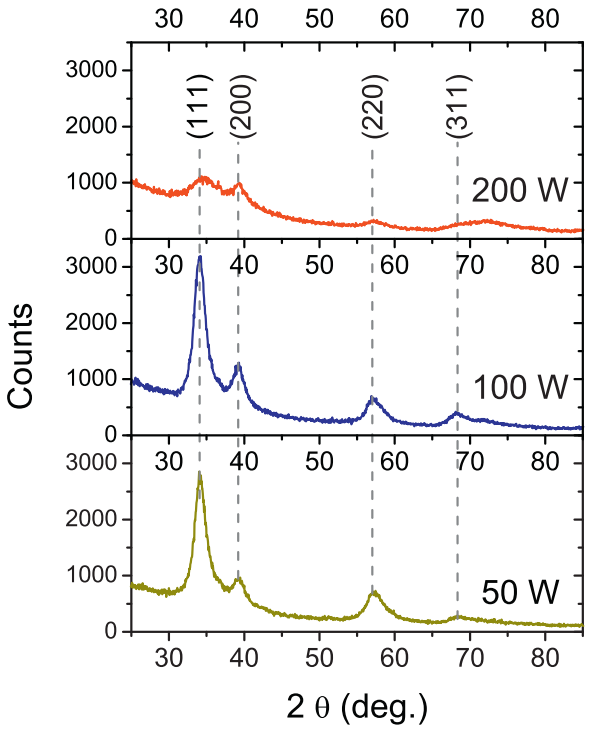

Fig. 1. X-ray diffraction pattern of iron mononitride (FeN) thin films prepared using magnetron sputtering using a power of 50 W, 100 W and 200 W.

b is an angular width in terms of 2θ, θ is the Bragg angle and λ is the wavelength of the radiation used. The values obtained for the grain size are given in Table 1. The average grain size calculated using (1 1 1) reflection is 5 nm for the samples prepared at sputtering power of 50 W and 100 W, while for the sample prepared at 200 W the grain size reduces significantly and the value obtained is 2.3 nm. This is somewhat surprising as it was expected that with an increase in the sputtering power a coarse grain structure should form as reported in case of Cu or Ni thin film prepared using different sputtering powers [37,40]. It is generally found that grain size increase with increasing sputtering power. This effect arises because with increase in sputtering power adatoms energy increases which results in their high mobility on the substrate surface and high surface diffusion which in helps in formation of a larger grain structure. However this may not be applicable in the present case as reactive sputtering is done in the present case (using only nitrogen to sputter iron) as compared to non-reactive sputtering reported in the literature. In case the number density of the atoms getting deposited on the substrate increases, they might colloid with the atoms condensing on the substrate and in this case the grain size may get restricted as observed in the present case.

In order to confirm the surface morphology of the deposited films, AFM measurements were carried out in the samples deposited using sputtering power of 100 and 200 W. Fig. 2 compares a typical AFM image of these samples. As can be seen from the AFM images the sample deposited using 200 W sputtering power

Table 1
XRD and neutron reflectivity parameters for iron nitride samples at different sputtering powers.

Parameter	50 W	100 W	200 W
a_{111} (±0.001 nm)	0.453	0.454	–
a_{200} (±0.001 nm)	0.459	0.459	–
a_{220} (±0.001 nm)	0.453	0.453	–
Grain size (±1 nm)	5	5	2.3
Interfacial roughness (±0.05nm)	2.1	2.2	0.9

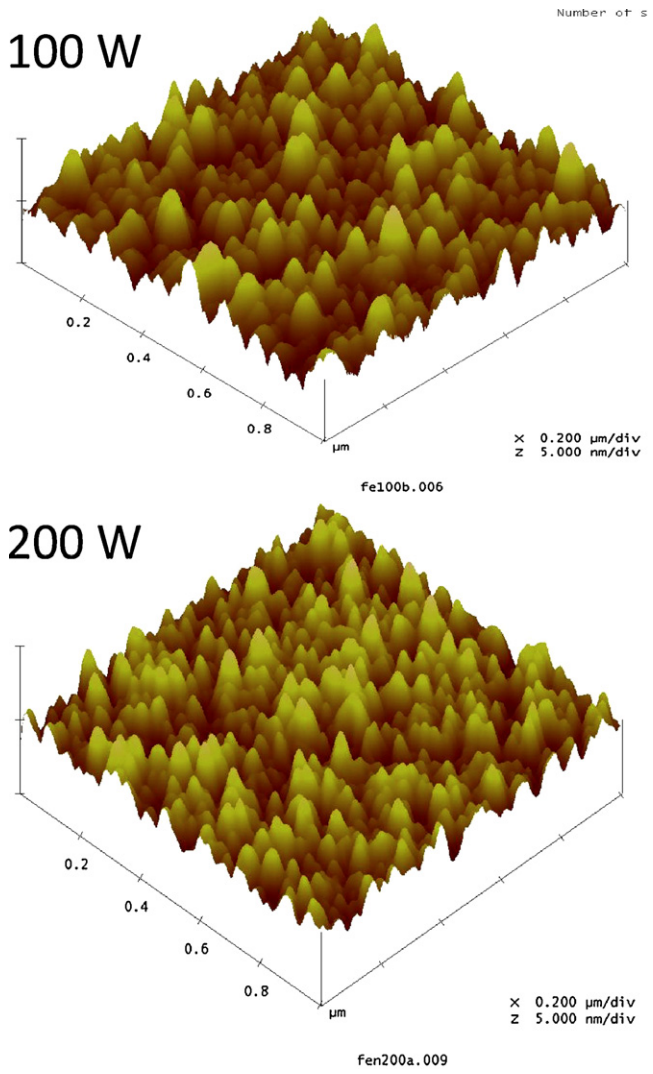

Fig. 2. AFM image of FeN thin films prepared using magnetron sputtering using a power 100 W and 200 W. The *x*, *y* and *z*-dimension in both images are same.

shows smaller and densely distributed grains as compared to the sample deposited using 100 W sputtering power. The observed results clearly support the XRD results.

The lattice constant was also deduced using the (2 0 0) and (2 2 0) reflections and are given in Table 1. As can be seen there, the lattice constant obtained using (1 1 1) and (2 2 0) is almost identical, however, the value obtained using (2 0 0) is 0.459 nm, which is slightly larger. This indicates that a small distortion may be present. The intensity ratio of the reflections $I_{(1\,1\,1)}/I_{(2\,0\,0)}$ has been used to confirm the structure. If the ratio $I_{(1\,1\,1)}/I_{(2\,0\,0)}$ is (>2) the ZnS-type structure formed while in case of NaCl-type structure this ratio should be smaller than unity (for $a = 0.450$ nm) [33]. Therefore, as can be deduced from the XRD patterns, our samples are single phase γ'''-FeN having ZnS type structure. This will be further confirmed in Section 3.3 where Mössbauer spectroscopy results are presented.

3.2. Neutron reflectivity

Fig. 3 shows the neutron reflectivity pattern of samples prepared at the sputtering power of 50, 100 and 200 W. The samples were in fact prepared in the form of an isotope multilayer with alternatively switching between Fe and ^{57}Fe enriched targets. Such multilayers have been used to study the self-diffusion of Fe using neutron reflectivity (NR) [41,42]. The composition of the samples as

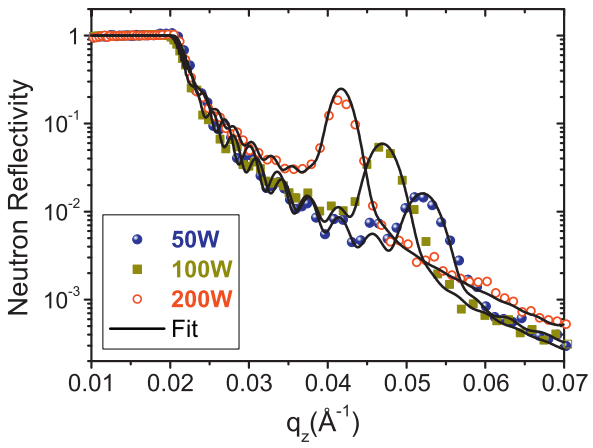

Fig. 3. Neutron reflectivity pattern of iron mononitride (FeN) thin films prepared using magnetron sputtering using a power of 50 W, 100 W and 200 W. The scattered points correspond to the measured experimental data and solid lines represent fit to them.

determined by fitting the neutron reflectivity data using a computer program [43] based on Parratt's formulism [44]:

(i) [Fe:N(9 nm)/^{57}Fe:N(4 nm)]$_{10}$ at 50 W
(ii) [Fe:N(10 nm)/^{57}Fe:N(4.7 nm)]$_{10}$ at 100 W
(iii) [Fe:N(12.4 nm)/^{57}Fe:N(5 nm)]$_{10}$ at 200 W

In order to fit the NR data we assumed that interfacial roughness of all Fe:N and ^{57}Fe:N layers is identical. The fitting parameters varied were interfacial roughness and bilayer thickness. As the power in the sputtering process is increased, the sputtering rate increases and the thickness of the film is increased. The fitting of the NR pattern gives the interfacial roughness of the samples which are given in the Table 1. We observe that the interfacial roughness of the sample prepared using 200 W sputtering power is significantly lower as compared to that of 50 and 100 W sample. This can be clearly seen in the Fig. 3, as the NR pattern for 200 W sample fall-off rather slowly as compared to 50 or 100 W sample. From our XRD and AFM measurements we observe a decrease in the grain size from 5 nm (for 50 or 100 W samples) to 2.3 nm for 200 W sample. A decrease in the grain size can lead to smoothness of the depositing thin film. The roughness of a thin film is caused due to topological morphology of the growing surface. It is expected that peaks and valleys form during the deposition and the shadowing of these peaks and valleys enhances the roughness [45]. As the grain size decreases, the structure becomes more isotropic and therefore the shadowing effects are minimized and lead to a reduction in the overall roughness.

3.3. Mössbauer spectroscopy

3.3.1. Room temperature CEMS

Fig. 4 shows the CEMS spectrum of iron nitride thin films prepared using a power of 50, 100 and 200 W. The obtained CEMS pattern is an asymmetric doublet in all the samples. Here we discuss the fitting procedure for the CEMS pattern. In the literature such CEMS pattern for non-magnetic iron nitrides has been obtained in a number of studies [24,26,27,33]. The fitting of such CEMS spectrum can either be done using two singlets or a singlet and a doublet [27]. In either case, the singlet with a lower value of the isomer shift (δ) was always assigned to ZnS-type FeN while the other subspectrum was argued to the vacancies in the ZnS-type FeN (2nd singlet) or due to presence of NaCl-type FeN (doublet). Therefore from the Mössbauer measurements alone, a precise assignment of subspectra can not be made.

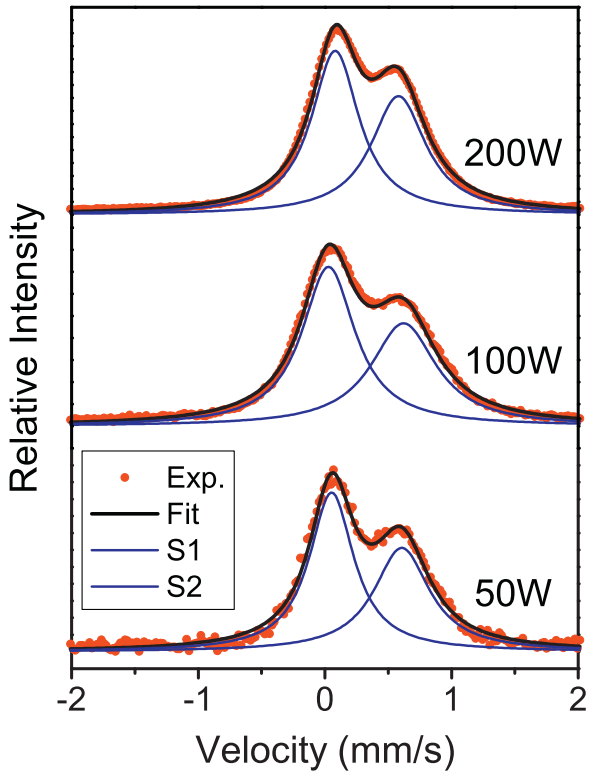

Fig. 4. Conversion electron Mössbauer spectroscopy (CEMS) pattern of iron mononitride (FeN) thin films prepared using magnetron sputtering using a power of 50 W, 100 W and 200 W. The scattered points correspond to the measured experimental data and solid lines represent fit to them.

From our XRD, data it is clear that the samples deposited at sputtering power of 50 and 100 W are single phase γ'''-FeN having ZnS type structure. Therefore, we assume that the Mössbauer spectrum can not be a mixture of γ''' and γ'' phases as reported in the literature [24,27,46]. This assumption is confirmed by low temperature and high field Mössbauer spectroscopy which are presented in the next section. Therefore to fit our CEMS spectrum we deconvolute it as two singlets: the singlet with the lower value of isomer shift ($\delta = 0.05$ mm/s) correspond to Fe coordinated tetrahedrally with four N atoms and the other singlet with $\delta = 0.6$ mm/s can be assigned to defects or vacancies in γ'''-FeN [21,33]. As we find out from the XRD measurements, the non-identical values of lattice constants indicates a distortion in the unit cell, and therefore presence of second singlet could be due to this distortion. The obtained fitted parameters from CEMS measurements are given in Table 2. Looking at the fitted CEMS values for samples deposited at 50, 100 and 200 W, we find that the values for three samples are almost identical. However, the XRD pattern and AFM images of the sample prepared at 200 W showed smaller grain size as compared to 50 or 100 W sample. This indicates that the local environment of the Fe atoms remained unaffected even though the grain size reduced. In order to further confirm the structure of our samples, low temperature and high field Mössbauer spectroscopy measurements were carried out and are presented in the next section.

Table 2
Conversion electron Mössbauer spectroscopy (CEMS) parameters for iron nitride samples at different sputtering powers.

Parameter	50 W	100 W	200 W
δ_{S1} (±0.002 mm/s)	0.05	0.03	0.08
δ_{S2} (±0.003 mm/s)	0.6	0.6	0.58
Area$_{S1}$ (±2%)	55	56	55
Area$_{S2}$ (±2%)	45	44	55

3.3.2. *Low temperature and high magnetic field Mössbauer spectroscopy*

Figs. 5 and 6 show the Mössbauer spectra of samples deposited at the sputtering power of 100 W and 200 W. These measurements were carried out in the same samples on which CEMS measurements were reported in the previous section. Since the samples were deposited on silicon substrate of thickness ~400 μm, it is possible to measure Mössbauer spectra in the transmission mode by allowing the γ-rays to pass through the silicon substrate. Fig. 5(a) shows room temperature Mössbauer spectra recorded in transmission mode and compares with those taken in conversion electron (reflection) geometry (see Fig. 4). The fitted parameters are similar in these two geometries.

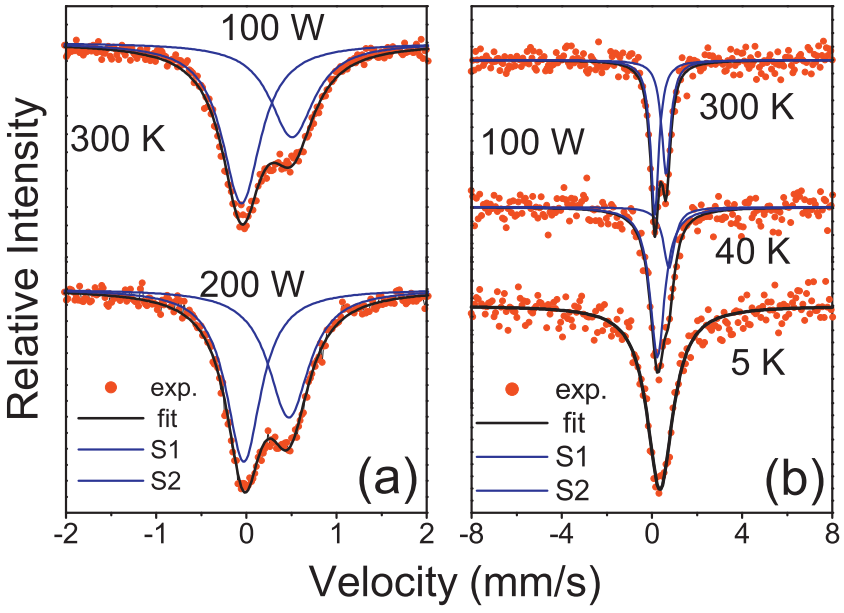

Fig. 5. Mössbauer spectroscopy (MS) pattern of iron mononitride (FeN) thin films prepared using magnetron sputtering using a power of 100 W and 200 W and measured at 300 K (a). The MS pattern of the 100 W sample measured at 300, 40 and 5 K (b).

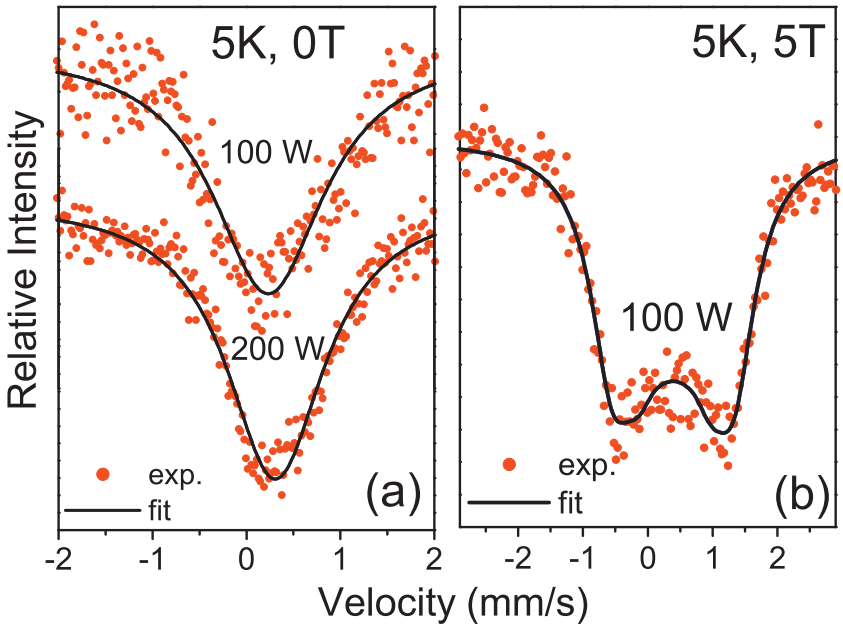

Fig. 6. Mössbauer spectroscopy (MS) pattern of iron mononitride (FeN) thin films prepared using magnetron sputtering using a power of 100 W and 200 W and measured at 5 K (a). The MS pattern of the 100 W sample measured at 5 K with an applied magnetic field of 5 T (b).

As discussed in the literature, Mössbauer spectra of sputter deposited iron mononitride always shows an asymmetric doublet. It was argued that the FeN phase with a lattice constant $a = 0.450$ nm is a mixture of NaCl-type (γ''') and ZnS-type (γ'') nitride. Whereas the phase with $a = 0.433$ nm is ZnS-type. The low temperature Mössbauer spectra of the phase with $a = 0.450$ nm shows magnetic splitting at 4.5 K [23]. It was argued that the component due to NaCl-type structure is magnetic while that with ZnS-type structure is non-magnetic at temperatures as low as 4.5 K. The hyperfine field of the NaCl-type magnetic component was as high at 49 T and when an external filed of 5 T is applied Fe magnetic moment does not change indicating that NaCl type iron nitride is an antiferromagnet with a very large hyperfine field [47].

The other phase with $a = 0.433$ nm remained non-magnetic even at 4.5 K. The main component in this structure originates due to Fe coordinated to four N neighbors. When an external field of 7 T was applied the magnitude of splitting observed was 7 T, indicating that ZnS-type iron nitride has no local magnetic moment [47].

With this overview of observed Mössbauer results in the literature, our results can be understood straightaway. When the samples prepared at sputtering power of 100 or 200 W were cooled down to 5 K (see Figs. 5 and 6), no magnetic splitting can be observed. Further even at 5 K there is no difference between the samples prepared at sputtering powers of 100 and 200 W. The observed behavior suggests that the samples are in the paramagnetic state at 5 K. The fitting of the data at 5 K reveals that the value of isomer shift is about 0.25 mm/s which is very close to the value of 0.21 mm/s obtained by Hinomura and Nasu for ZnS-type $FeN_{0.91}$ [47].

Further we applied an external field of 5 T to observe changes in the magnetic moment. The Mössbauer spectrum measured at 5 K under an applied field of 5 T is shown in Fig. 6. We observed that with an applied field of 5 T the Mössbauer spectrum gets splitting amounting to 5 T, the same as that of applied magnetic field. This indicates that there is no local magnetic moment in our samples. Therefore from our low temperature and high field Mössbauer spectroscopy measurements it can be confirmed that our samples are ZnS-type γ'''-FeN with a lattice constant $a = 0.453$ nm. This confirms recent results obtained in the literature [27,33].

3.3.3. Annealing behavior

We also measured the thermal stability of samples prepared at sputtering power of 100 W and 200 W using conversion electron Mössbauer spectroscopy. Since both these sample behave similarly the results of the sample deposited at sputtering power of 100 W are presented in Fig. 7. The CEMS measurements were carried out on the sample annealed in a vacuum furnace pumped down to 1×10^{-6} mbar. The annealing was done at temperatures of 423 K, 523 K, and 623 K for 2 hours at each temperatures. The pressure during annealing was typically $2–3 \times 10^{-6}$ mbar. As can be seen from the Fig. 6 the CEMS spectra does not show any

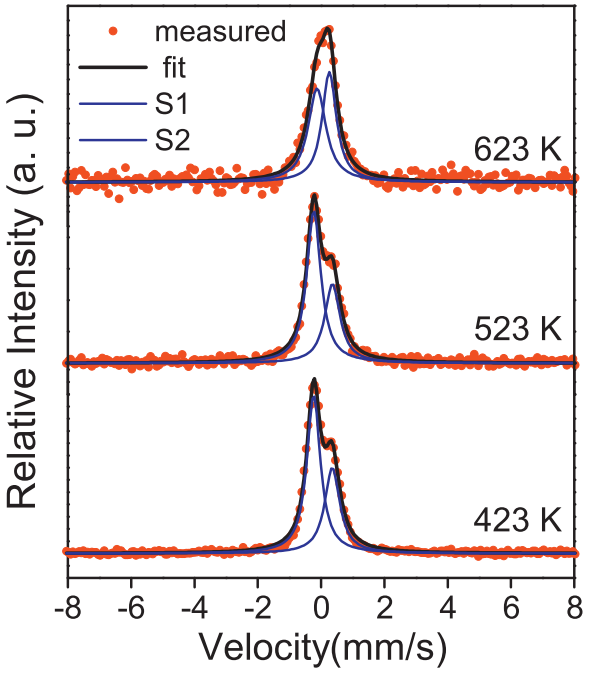

Fig. 7. Conversion electron Mössbauer spectroscopy (CEMS) pattern FeN thin films prepared using a sputtering power of 100 W and after annealing 423, 523 and 623 K.

appreciable changes in the spectra as the annealing temperature is increased. Since no magnetic splitting can be observed, it confirms that the nonmagnetic FeN phase is stable even up to 623 K. The observed spectra are fitted using two singlets as discussed previously. The obtained values of isomer shifts for the sample annealed at 423 K is (δ_{S1} = 0.1 mm/s) and (δ_{S2} = 0.7 mm/s) their relative area ratio is ($Area_{S1}$: $Area_{S2}$ = 62:37). These values remain almost same at annealing temperature of 523 K. However after annealing at 623 K, the line width increases and the isomer shift of singlet *S*1 increases to 0.2 mm/s while that of *S*2 decreases to 0.6 mm/s, and the relative area ratio becomes ($Area_{S1}$: $Area_{S2}$ = 48 : 52).

4. Conclusion

In conclusion, we deposited single phase iron mononitride thin films using nitrogen alone as a sputtering gas at different deposition rates. The structure of the samples as found from XRD and low temperature high magnetic field Mössbauer spectroscopy measurements is γ'''-FeN with ZnS-type structure. It was found that an increase in the deposition rates due to increase in sputtering power results in a more disordered crystal structure however, the local environment of Fe atoms remains unaffected with an increase in the deposition rates. The neutron reflectivity and AFM measurements suggests that the overall roughness of the deposited film decrease with an increase in sputtering power. As the grain size decreases, the structure becomes more isotropic and therefore the shadowing effects are minimized and lead to a reduction in the overall roughness.

From our work it can be clearly seen that the sputtering of iron targets with pure nitrogen gas yields single phase iron mononitride thin films. By varying the sputtering power, the long range ordering can be controlled although the local structure of the samples remains unaffected by a variation in sputtering power.

Acknowledgments

We acknowledge DST for providing financial support to carry out NR experiments under its scheme 'Utilization of International Synchrotron Radiation and Neutron Scattering facilities'. A part of this work was performed under the Indo Swiss Joint Research Programme with grant no. INT/SWISS/JUAF(9)/2009. We are thankful to Dr. P. Chaddah for continuous support and encouragement.

References

[1] J.M.D. Coey, P.A.I. Smith, J. Magn. Magn. Mat. 200 (1999) 405–424.
[2] P. Schaaf, Prog. Mater. Sci. 47 (2002) 1–161.
[3] K.H. Jack, J. Alloys Compds. 222 (1951) 160–166.
[4] K.H. Jack, Proc. Roy. Soc. A 208 (1951) 216.
[5] N. Kardonina, A. Yurovskikh, A. Kolpakov, Met. Sci. Heat Treat. 52 (2011) 457–467.
[6] T.K. Kim, M. Takahashi, Appl. Phys. Lett. 20 (1972) 492.
[7] M. Komuro, Y. Kozono, M. Hanazono, Y. Sugita, J. Appl. Phys. 67 (1990) 5126–5130.
[8] S. Atiq, H.S. Ko, S.A. Siddiqi, S.C. Shin, J. Alloys Compds. 479 (2009) 755–758.
[9] C. Navío, J. Alvarez, M.J. Capitán, D. Ecija, J.S. Gallego, F. Ynduráin, R. Miranda, Phys. Rev. B 75 (2007) 125422.
[10] C. Navío, J. Alvarez, M.J. Capitan, J. Camarero, R. Miranda, Appl. Phys. Lett. 94 (2009) 263112.
[11] C. Navío, J. Alvarez, M.J. Capitan, F. Ynduráin, R. Miranda, Phys. Rev. B 78 (2008) 155417.
[12] L. de Wit, T. Weber, J.S. Custer, F.W. Saris, Phys. Rev. Lett. 72 (1994) 3835.
[13] J.M. Gallego, D.O. Boerma, R. Miranda, F. Ynduráin, Phys. Rev. Lett. 95 (2005) 136102.
[14] H. Jacobs, D. Rechenbach, U. Zachwieja, J. Alloys Compds. 227 (1995) 10–17.
[15] D. Rechenbach, H. Jacobs, J. Alloys Compds. 235 (1996) 15–22.
[16] V. Demange, T.H. Loi, P. Weisbecker, E. Bauer-Grosse, Thin Solid Films 494 (2006) 184–189.
[17] J.M. Gallego, S.Yu. Grachev, D.M. Borsa, D.O. Boerma, D. Écija, R. Miranda, Phys. Rev. B 70 (2004) 115417.
[18] W.Y. Ching, Y.N. Xu, P. Rulis, Appl. Phys. Lett. 80 (2002) 2904.
[19] Y.N. Xu, P. Rulis, W.Y. Ching, J. Appl. Phys. 91 (2002) 7352.
[20] A. Oueldennaoua, E. Bauer-Grosse, M. Foos, C. Frantz, Scripta Metall. 19 (1985) 1503.
[21] H. Nakagawa, S. Nasu, H. Fujii, M. Takahashi, F. Kanamaru, Hyp. Interact. 69 (1991) 455.
[22] K. Suzuki, H. Morita, T. Kaneko, H. Yoshida, H. Fujimori, J. Alloys Compds. 201 (1993) 11.
[23] T. Hinomura, S. Nasu, Phys. B: Cond. Matter 237–238 (1997) 557.
[24] L. Rissanen, M. Neubauer, K.P. Lieb, P. Schaaf, J. Alloys Compds. 274 (1998) 74.
[25] M. Gupta, A. Gupta, P. Bhattacharya, P. Misra, L.M. Kukreja, J. Alloys Compds. 326 (2001) 265.
[26] M. Gupta, A. Gupta, S. Rajagopalan, A.K. Tyagi, Phys. Rev. B 65 (2002) 214204.
[27] D.M. Borsa, D.O. Boerma, Hyp. Interact. 151–152 (2003) 31–48.
[28] X. Wang, W.T. Zheng, H.W. Tian, S.S. Yu, W. Xu, S.H. Meng, X.D. He, J.C. Han, C.Q. Sun, B.K. Tay, Appl. Surf. Sci. 220 (2003) 30–39.
[29] R. Gupta, M. Gupta, Phys. Rev. B 72 (2005) 024202.
[30] E.B. Bradley, Th. Buhrmester, J.R. Dahn, Thin Solid Films 493 (2005) 60–66.
[31] E. Andrzejewska, R. Gonzalez-Arrabal, D. Borsa, D.O. Boerma, Nucl. Instr. Methods Phys. Res. B 249 (2006) 838–842.
[32] W. Lin, J. Pak, D.C. Ingram, A.R. Smith, J. Alloys Compds. 463 (2008) 257–262.
[33] I. Jouanny, P. Weisbecker, V. Demange, M. Grafouté, O. Peña, F. Bauer-Grosse, Thin Solid Films 518 (2010) 1883.
[34] C. Navío, M.J. Capitán, J. Álvarez, R. Miranda, F. Ynduráin, New J. Phys. 12 (2010) 073004.
[35] A. Filippetti, W.E. Pickett, Phys. Rev. B 59 (1999) 8397–84009.
[36] M.S. Miao, P. Lukashev, A. Herwadkar, W.R.L. Lambrecht, Phys. Stat. Slo. (c) 2 (2005) 2516–2519.
[37] K.Y. Chan, B.S. Teo, J. Mater. Sci. 40 (2005) 5971–5981.
[38] M. Gupta, T. Gutberlet, J. Stahn, P. Keller, D. Clemens, Pramana J. Phys. 63 (2004) 57.
[39] B.D. Cullity, Elements of X-ray Diffraction, Addison-Wesley, MA, 1978.
[40] B.G. Priyadarshini, S. Aich, M. Chakraborty, J. Mater. Sci. 46 (2011) 2860–2873.
[41] M. Gupta, A. Gupta, J. Stahn, M. Horisberger, T. Gutberlet, P. Allenspach, Phys. Rev. B 70 (2004) 184206.
[42] M. Gupta, A. Gupta, S. Chakravarty, R. Gupta, T. Gutberlet, Phys. Rev. B 74 (2006) 104203.
[43] C. Braun, Parratt32 – The Reflectivity Tool (1997–1999) HMI Berlin.
[44] L.G. Parratt, Phys. Rev. 95 (1954) 359–369.
[45] M. Gupta, J. Appl. Phys. 98 (2005) 064305.
[46] P. Schaaf, C. Illgner, M. Niederdrenk, K.P. Lieb, Hyp. Interact. 95 (1995) 199.
[47] T. Hinomura, S. Nasu, Hyp. Interact. 111 (1998) 221–226.